NANO LETTERS

Letter

pubs.acs.org/NanoLett

Current–Voltage Characterization of Individual As-Grown Nanowires Using a Scanning Tunneling Microscope

Rainer Timm,* Olof Persson, David L. J. Engberg, Alexander Fian,† James L. Webb, Jesper Wallentin,‡ Andreas Jönsson, Magnus T. Borgström, Lars Samuelson, and Anders Mikkelsen

The Nanometer Structure Consortium, Department of Physics, Lund University, P.O. Box 118, 221 00 Lund, Sweden

Supporting Information

ABSTRACT: Utilizing semiconductor nanowires for (opto)-electronics requires exact knowledge of their current–voltage properties. We report accurate on-top imaging and *I*–*V* characterization of individual as-grown nanowires, using a subnanometer resolution scanning tunneling microscope with no need for additional microscopy tools, thus allowing versatile application. We form Ohmic contacts to InP and InAs nanowires without any sample processing, followed by quantitative measurements of diameter dependent *I*–*V* properties with a very small spread in measured values compared to standard techniques.

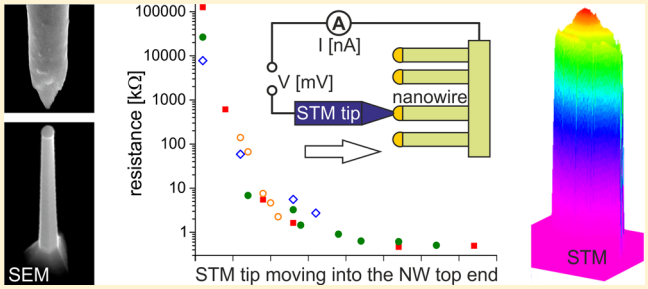

KEYWORDS: *Semiconductor nanowire, scanning tunneling microscopy, Ohmic contact, nanowire contacts, resistivity*

The development of high-performance/low cost photovoltaic devices, light-emitting diodes with optimal color-rendering index, and high-speed/low-power electronics for mobile applications are three important areas in modern society where novel semiconductor nanowire structures are expected to lead to qualitative advances in performance.[1−4] In addition, these new structures are exploratory systems for new physical phenomena such as Majorana fermions[5,6] and exciton dynamics.[7,8] Free-standing semiconductor nanowires in particular offer advantages such as atomically precise heterostructures in a wide range of materials[9,10] and the epitaxial combination of III–V semiconductors with Si.[4,11]

However, for the successful realization of future nanowire applications it is crucial to study how the resistivity and exact *I*–*V* behavior of individual nanowires determine the performance of the entire device. Unfortunately, these parameters cannot be predicted from known bulk parameters and will depend strongly on the nanowire surface.[12,13] Even more problematic, most methods that measure these quantities in a reliable and reproducible fashion in bulk materials do not work for the nanowire geometry. This has led to a significant effort to develop specialized methods for characterizing nanowire electronic properties.[14−18] The most commonly used approach to investigate transport properties of individual nanowires uses a nanowire field-effect transistor (FET) geometry where the nanowires are deposited on an insulating substrate and contacted with metal electrodes defined by electron beam lithography (EBL).[19,20] There are three significant limitations with this method. First, the resulting *I*–*V* characteristics are often dominated by the contact between the nanowire and the metal electrodes, rather than the nanowire itself.[21−25] Second, data from broken nanowires in FET geometry are not directly comparable with nanowire devices in an upright-standing configuration.[26,27] Third, the significant number of processing steps is time-consuming and strongly limits the versatility of surface treatment and shell layer design that is inherent to free-standing nanowires.

A more direct concept for measuring single nanowire resistivity is to establish a point contact between a metallic nanoprobe and the top end of an upright standing as-grown nanowire. This approach requires no extra processing, and it provides an epitaxial and therewith well-defined back contact to the individual nanowire. Talin and co-workers have recently revealed exciting new insights in transport properties of nanowires by positioning a W nanoprobe inside a scanning electron microscope (SEM) for studying the *I*–*V*-characteristics of individual Ge,[28] GaN,[29] InAs,[30] or GaAs[31] nanowires. Comparable investigations have also been reported by Kavanagh and co-workers for GaAs[32] and InN[33] nanowires. While these revealed the device morphology and geometry, the precise structure on top of the nanowire prior to contacting was not known. Here it should be noted that the exact structural properties of the contacting area have a large impact on the results from such contact measurements.[34,35] Alternatively, the nanoprobe can be placed within a transmission electron microscope (TEM), enabling precise positioning, though under the nontrivial limitations of the tight TEM geometry and elaborate sample processing. However, independent realizations of such a setup found it very challenging,[36,37] if possible at all,[38] to establish an Ohmic contact between the

Received: July 12, 2013
Revised: September 5, 2013
Published: September 23, 2013

   dx.doi.org/10.1021/nl402570u | *Nano Lett.* 2013, 13, 5182–5189

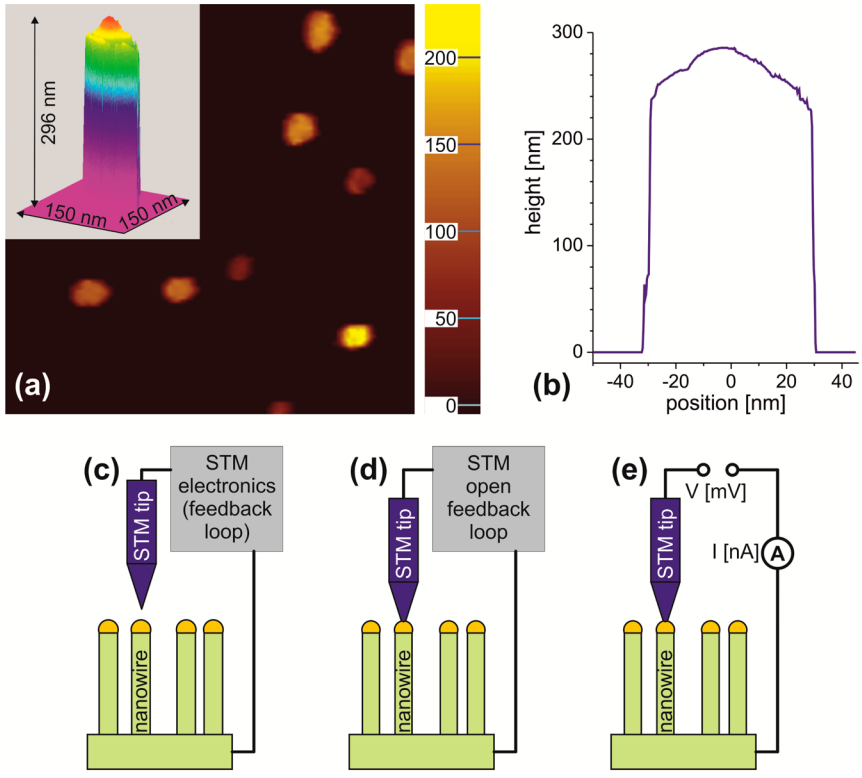

Figure 1. (a) The 1 μm × 1 μm STM overview image of upright standing InAs nanowires, obtained with a sample bias of $V = -0.5$ V and a tunneling current of $I = 100$ pA. The actual length of the nanowires is about 2 μm, but the z position of the STM tip is restricted, so that it cannot reach down to the substrate. Therefore the color scale of the STM image corresponds to relative length differences of individual nanowires, indicated in nm. The inset shows a 3D close-view STM image of a single nanowire. (b) STM height profile of the nanowire shown in the inset of (a). Note that the bottom height is determined by the restricted z range of the STM tip and not by the sample. The position and diameter of the nanowire and the shape of the Au particle on top can be obtained with subnm resolution. (c–e) Sketch of the procedure for measuring the resistivity of individual nanowires. (c) First, the exact position and shape of a nanowire is determined by imaging with the STM in top-view geometry. (d) Then, the STM feedback loop is interrupted and the tip is further approached toward the nanowire and slightly pushed into the center of the metal particle on top of the nanowire in a gentle and controlled way, establishing an Ohmic point contact between the tip and the nanowire. (e) Finally, an external current preamplifier is connected to measure the I–V properties of the contacted nanowire.

nanowire and the nanoprobe, which was related to oxidation of the nanoprobe and to carbon contamination induced by the electron beam.[36] Thus, the main challenges for nanoprobe I–V measurements at single nanowires are (i) the exact positioning of the nanoprobe toward the nanowire, (ii) to provide proper surface conditions of both the nanowire and the probe, which are crucial for establishing a well-defined system, and (iii) to keep the method versatile.

Here, we take the nanoprobe concept a qualitative step further and use the scanning tunneling microscope (STM) tip for both imaging individual upright standing nanowires and for measuring their electrical properties after establishing a point contact. By performing scanning tunneling microscopy on upright standing nanowires, which is an unconventional, though successfully proven geometry,[39] we completely remove the need for an electron microscope during the measurements. This setup (i) gives the unique subnanometer resolution of the STM, (ii) works in an ultrahigh vacuum (UHV) surrounding that implies control over the surface conditions of sample and probe, and (iii) it can be realized with only a standard STM and without any sample processing, being the most direct realization of the nanoprobe concept. We present first results on homogeneous InP and InAs nanowires where we have imaged the top end of the nanowires with subnm resolution and routinely obtained Ohmic contacts between the probe tip and individual nanowires with a contact resistance of less than 22 Ω. Measured nanowire resistances R are inversely proportional to the cross-sectional area for nanowires in a diameter range of 50–170 nm, as expected. The key prerequisites for the extremely low contact resistance are oxide-free surfaces enabled by UHV probe treatment and knowledge of the exact topography on top of the nanowires, since this can significantly influence the point contact formation.[34] While it might seem surprising that the inherently 2D STM technique can be used to image structures with such a high aspect ratio as that of upright standing nanowires, once this conceptual barrier has been overcome this opens up new radical opportunities in the study of nanowire devices.

All nanowires studied here were grown by molecular vapor phase epitaxy (MOVPE).[40] Au nanoparticles were randomly distributed on the growth substrate using an aerosol technique, initiating nanowire growth via the vapor–liquid–solid mode. Trimethylindium ($(CH_3)_3In$), phosphine (PH_3), and hydrogen sulfide (H_2S) were used as precursors with molar fractions of 3.5×10^{-6}, 6.25×10^{-3}, and 2.4×10^{-8} for growing highly S-doped InP nanowires at 420 °C on an n-doped InP (111)B substrate, as described in more detail in ref 41. InAs nanowires were grown on an n-doped InAs (111)B substrate using triethylindium ($(C_2H_5)_3In$) and arsine (AsH_3) in two growth steps: The lower part of the nanowires was Si-doped, while the upper part remained without intentional doping. After growth, the nanowire samples were exposed to air during storage until

dx.doi.org/10.1021/nl402570u | Nano Lett. 2013, 13, 5182–5189

they were loaded without any further processing or treatment into the UHV STM chamber. STM measurements were performed in constant current mode using a JEOL JSTM-4500 XT microscope with an RHK SPM 100 control unit, bypassed with an external sample voltage supply, and the RHK XPMPro software. The STM was operated at room temperature at a base pressure below 10^{-9} mbar. STM tips were made of 0.25 mm thick W wire by electrochemical etching in either KOH or NaOH solution, followed by Ar^+ ion sputtering at 2 to 3 keV within the UHV chamber of the STM. In some cases, the W wire was annealed in vacuum prior to the etching step, resulting in STM tips with a slightly higher aspect ratio, which however did not seem to affect the electrical measurements. *I*−*V* spectra of individual contacted nanowires were acquired using a Stanford Research Systems SR830 Lock-In Amplifier as a programmable voltage source and a Stanford Research Systems SR570 Current Preamplifier coupled with a Hewlett-Packard HP34401A Multimeter, synchronized using a custom written Labview program.

The procedure used here for current−voltage measurements of individual semiconductor nanowires is sketched in Figure 1. First, the upright standing nanowires are imaged by STM, which is a nonconventional and challenging task, that nevertheless can be realized even with a standard STM. In order not to damage the nanowires or the probe tip, the STM tip is initially approached toward the sample in an iterative procedure, until the top end of one or several nanowires is imaged, as shown in Figure 1a−c. This process is described in more detail in ref 39. For most nanowires studied here, the nanowire length exceeds the height range of the STM (450 nm), so that the STM tip scans across the top end of the nanowires, but does not reach the sample surface of the growth substrate. This results in an STM overview image like the one shown in Figure 1a, where several nanowires exhibit a different height contrast corresponding to the relative difference in the nanowire length. It should be noticed that by this approach even a native oxide layer on the nanowire sample will not affect the STM measurements, since the STM tip does not reach the oxidized sample substrate but only the top end of the nanowires, which usually consists of a metal nanoparticle. One specific nanowire can be chosen for characterization and a zoomed-in STM image of that nanowire can be taken, as shown in the inset of Figure 1a. From the STM height profile displayed in Figure 1b, it can be seen that the nanowire diameter and the exact topography of its top end can be obtained with subnanometer resolution. With this information, the STM tip can be positioned exactly at the center of the upright standing nanowire, where the point contact has to be established. Now the constant-current feedback loop of the STM has to be interrupted, so that the tip can be further approached toward the nanowire until a point contact is reached (Figure 1d), which is detected by a sudden increase of the measured current. This current typically exceeds the saturation limit of the STM electronics, so that the connection for current read-out is switched to a secondary current amplifier with a larger range (Figure 1e).

Nanowires of different III−V semiconductor materials like InP and InAs have been contacted and measured by our method. All nanowires studied were grown in the particle assisted growth mode using catalytic Au nanoparticles, which upon growth form Au−In alloys. This leads to a well-defined situation where a point contact is formed between the Au−In particle and the STM tip, which is made of etched tungsten wire and has been sputtered within UHV, meaning that two clean and completely oxide-free metals are brought into contact.

The nanowires studied here had diameters between 50 and 170 nm, determined by the size of the original Au seed particle, although the method could well be applied to thinner or thicker nanowires as well. An SEM image of a typical nanowire can be seen in Figure 2a. The diameters of the nanowires are in the same range as the width of the STM probe tip, which routinely reaches a radius of curvature of less than 30 nm, as can be seen in the SEM image of a typical STM tip shown in Figure 2b. Thus, the process of forming a point contact can be understood as a sharp, stiff W tip penetrating into the comparably soft, spherical metal particle on top of the nanowire.

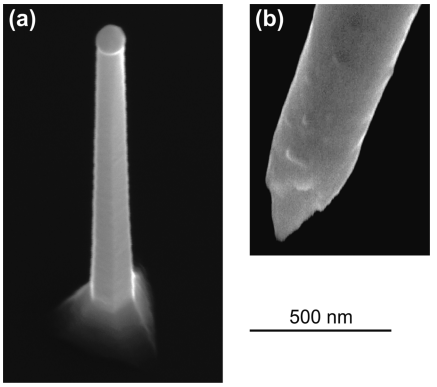

Figure 2. SEM images of (a) an InP nanowire and (b) an STM probe tip made of vacuum-annealed W wire after etching in KOH solution and sputtering using Ar+ ions. The image in (a) was acquired with a tilt angle of 15°. The scale bar is valid for both images.

With the gentle and controlled alignment of the piezo positioners holding the STM tip, the process of point contact formation can be monitored, as shown in Figure 3. At the first, very weak contact between a sharp STM tip and the metal particle on top of the nanowire, usually a strongly nonlinear *I*−*V* spectrum with a very small current in the nanoamperes range is measured, as shown in Figure 3b. These very small currents are typical for tunneling through a remaining thin vacuum barrier. When the tip is pushed slightly further into the metal particle using nanometer-sized steps, the measured current typically increases with each step (Figure 3c), until a point where it increases significantly and the *I*−*V* curve becomes linear (Figure 3d), indicating that an Ohmic contact has formed. This behavior can be explained by the geometrical cross-section of the point contact. When the very sharp tip touches the metal particle at the initial contact, the very small cross-section does not enable a sufficient current density. With each small step that the piezo positioner pushes the tip further into the Au−In particle, the contact cross-section increases and its resistance decreases, until the cross-section is not limiting the current flow anymore and an Ohmic contact has formed.

According to Figure 3, between 10 and 15 steps by our piezo positioner are typically needed for establishing an Ohmic contact with a sharp tip. One piezo step corresponds to a tip movement of about 5 nm if the tip can move freely. This step size would give an astonishingly large value for the necessary tip-nanowire positioning. However, we have observed previously that free-standing nanowires are flexible, even in their axial direction, so that the attractive electrostatic force between

dx.doi.org/10.1021/nl402570u | *Nano Lett.* 2013, 13, 5182−5189

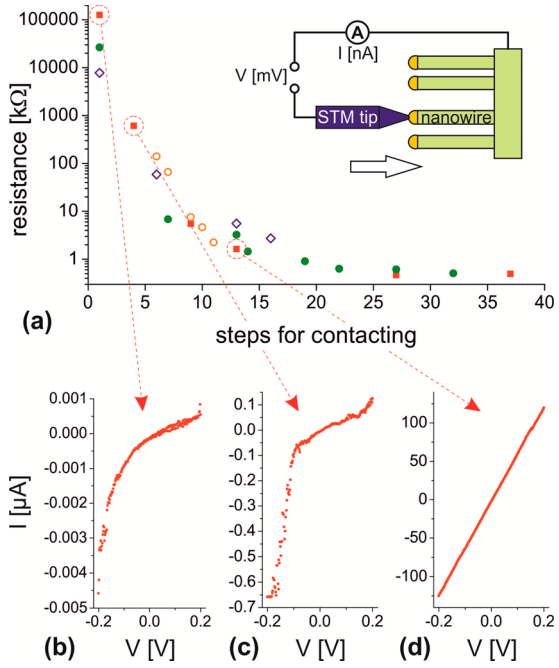

Figure 3. Formation of an Ohmic contact between the probe tip and the nanowire: (a) Change of the measured resistance of four individual nanowires when the probe tip is gently pushed by small steps into the metal seed particle on top of the nanowire, as shown schematically in the inset. Red filled squares, blue open diamonds, green filled circles, and orange open circles correspond to one of the four nanowires, respectively. (b–d) $I-V$ curves measured at one of the nanowires after pushing the tip (b) 1, (c) 4, and (d) 13 steps into the metal particle. The resistance values plotted in (a) correspond to the averaged slope of the $I-V$ spectra.

a biased STM tip and a nanowire can cause the nanowire to stretch several tens of nanometers or by more than 1% of its length when forming the initial point contact.[39] The nanowire can come back to its initial length when the STM tip is pushed forward. Thus, we assume that the movement of the STM tip is mostly compensated by a contracting nanowire, so that the observed 10 to 15 steps for forming the Ohmic contact probably correspond to a penetration depth of the tip into the Au–In particle of around 10 nm. It should be noted that these 10 to 15 steps are typical for freshly prepared, sharp tips, where the initial point contact can be assumed to consist of only a few atoms, while rather blunt tips have been found to form Ohmic contacts already after one or two steps, which however does not influence the measured $I-V$ properties once the contact has formed. This behavior confirms that a sufficiently large contact cross-section is necessary for the Ohmic contact, also in agreement with other nanoprobe experiments reported in literature.[30] We note that upon contact, currents up to 30 μA (at 0.1 V) were measured in a single nanowire. Such high currents might explain the need for a sufficiently large contact cross-section. On the other hand, nanowires with Au particle diameters down to 20 nm have successfully been contacted by this method, giving an upper limit of the necessary contact cross-section of a few nanometers.

After establishing an Ohmic contact, the tip can be pushed even further into the metal particle, which will create strain and cause bending of the nanowire,[36] thereby changing its intrinsic resistivity. Correspondingly, a very small further decrease of the measured resistance can be seen in Figure 3 at these conditions.

In the following, the slope of the first linear $I-V$-curve upon contacting a nanowire with the STM tip, which usually comes along with a strong increase of the measured current, will be assigned to be the resistance of this specific nanowire.[42]

Considering the high currents measured in single nanowires, corresponding current densities of up to 0.6×10^6 A/cm^2 were obtained. This could potentially lead to heating of the device. We can however repeat $I(V)$ measurements over time periods varying between minutes and hours and with different duration of the $I(V)$ measurement itself with reproducible results. In addition, the effect of carrier transport on temperature in nanowires has been calculated, indicating that even for four times as large current densities as used in our experiments, the temperatures should not go above 250 °C.[43]

In order to test our method, we chose to study highly doped nanowires, where a significant series resistance induced by the contacts would strongly influence the measured $I-V$ properties. We used InP nanowires with diameters around 100 nm and lengths of about 2 μm that were n-doped using H_2S.[41] An SEM image of such a nanowire is shown in Figure 2a. Resistance measurements on 14 individual nanowires on this sample are presented in the left part of Figure 4a. All these nanowires showed linear $I-V$ curves like the one plotted as blue curve in Figure 4c. The resulting average resistance was R = 4.3 (±2.2) kΩ.

As a direct comparison, we made several attempts to measure nanowires from the same sample in the traditional FET configuration. Here the nanowires were mechanically transferred to a degenerately doped silicon substrate, which was covered with 100 nm of SiO_2 and 10 nm of HfO_2. The position of the nanowires was measured in an optical microscope and after resist deposition contacts were created to selected nanowires by EBL and metal lift off, using a Ti/Pd metal combination. However, the observed $I-V$ curves, like the one plotted in green in Figure 4c, were non-Ohmic, and completely dominated by contacts with Schottky-like barriers. We assume these problems in externally contacting the nanowires to result from the oxidized nanowire surface, demonstrating the advantage of our STM-based method for $I-V$ measurements with oxide-free and thus low-resistive contacts.

Since the as-grown nanowire sample had been exposed to ambient air before being transferred into the STM, the measured resistivity may be influenced by the highly n-doped shell around the nanowire, for example, an $In_xP_yO_z$ layer.[44] It is well-known that surface chemistry and structure can potentially influence nanowire properties.[45] In order to investigate this possibility, we etched the InP nanowire sample in phosphoric acid and sulfuric acid, followed by surface passivation using ammonium sulfide,[22] and immediately transferred them back into the UHV environment of the STM. Resistance measurements on five individual, freshly etched nanowires are shown in the right part of Figure 4a, resulting in an average nanowire resistance of R = 4.2 (±2.5) kΩ, which is the same value as before the etching procedure. This indicates that the observed conductance is related to the InP nanowires themselves and not to the thickness of a shell layer. It should be noticed, however, that only an almost total removal of the surface oxides will seriously affect the surface pinning in the case of InP nanowires, as we have shown before.[44]

A significant spread of the measured resistance R among different individual nanowires is observed, as can be seen in Figure 4a,b. The large spread can be explained by the variation of the nanowire diameter. From the STM images, which are

dx.doi.org/10.1021/nl402570u | Nano Lett. 2013, 13, 5182–5189

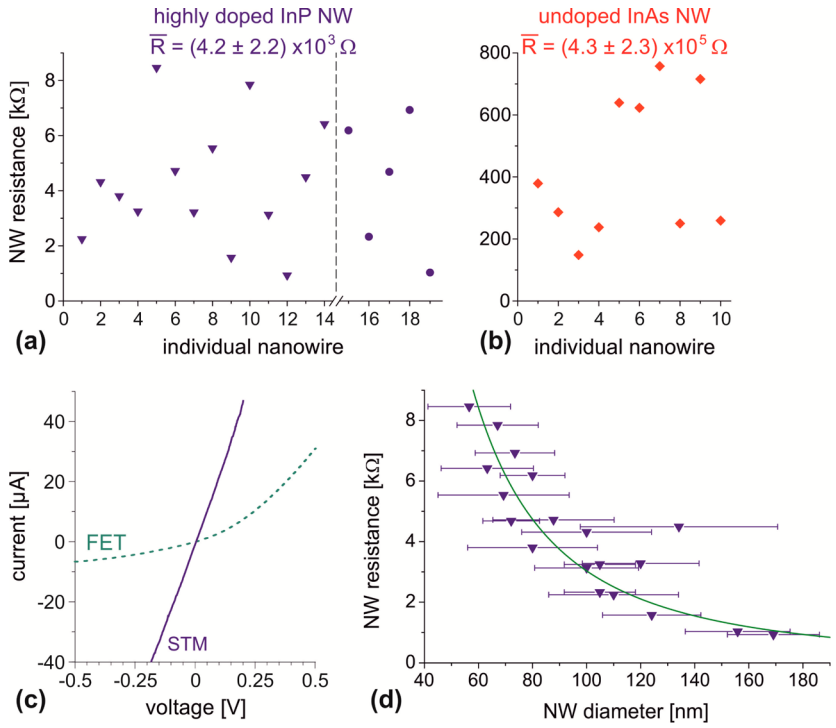

Figure 4. Measured resistance properties of individual nanowires, as obtained from linear $I-V$-spectra. (a) Resistance of highly doped InP nanowires. The data in the left part (triangles) corresponds to as-grown nanowires and the data in the right part (circles) to nanowires from the same sample after etching and surface passivation. (b) Resistance of nonintentionally doped InAs nanowires. The average resistance and standard deviation for the corresponding nanowires is indicated in (a) and (b). (c) Typical $I-V$ curves of an individual InP nanowire obtained with the STM tip in point contact (blue, straight line) and in an FET geometry reference experiment using EBL-defined contacts (dark green, dotted line). The linear nanowire behavior can clearly be seen in the STM-based data, while the reference experiment fails in providing Ohmic contacts. (d) Resistance of the same nanowires as shown in (a), here plotted over the diameter, which is determined for each nanowire from the STM images. The experimental uncertainty of the diameter measurement, mostly due to the convolution with the STM tip shape, is indicated by error bars. A simple fit of the experimental data is shown by the green line, confirming the dependence of the nanowire resistance R on the diameter d with $R = 30.3\ \mathrm{k\Omega\ nm^2}/d^2$.

taken to characterize a nanowire and its surroundings prior to contacting it, the nanowire diameter can be estimated. To estimate this from the images, the convolution of nanowire and tip shape in the STM image needs to be considered, especially if the tip has already been used for contacting one or several other nanowires before. Figure 4d shows the resistance of the highly doped InP nanowires plotted over their diameter with error bars indicating the estimated uncertainty of the shape measurements. The clear decrease of the resistance R with increasing nanowire diameter d agrees well with a classical resistance behavior of $R \sim 1/d^2$ (since confinement effects should play only a minor role at the given diameters). Considering the measured nanowire diameters and assuming a constant length of 2 μm, a resistivity $\rho = 13.3\ (\pm 5.3)\ \Omega\ \mu$m was obtained for the individual nanowires. The resistivity is determined by the charge carrier density n and their mobility μ by $\rho = (ne\mu)^{-1}$ with the elementary charge e. If we assume a mobility $\mu = 400\ \mathrm{cm^2\ V^{-1}\ s^{-1}}$, as was recently measured for similar H_2S-doped InP nanowires,[41] the resistivity corresponds to a dopant concentration $n = 1.2 \times 10^{19}\ \mathrm{cm^{-3}}$.

One might ask whether the actual resistivity of the nanowires could be even lower and if a part of the measured resistivity is due to the contacts. We can exclude any significant resistance from the growth substrate and its back contact, since the InP nanowires are grown epitaxially on a highly n-doped InP (111) B wafer, resulting in a single-crystalline interface. In order to evaluate the resistivity of the point contact between the STM tip and the nanowire, we performed a first reference measurement by establishing a point contact between the tip and the nanowire growth substrate at various substrate positions, both between nanowires and at areas of the substrate where no nanowires had been grown, obtaining an average resistance of $R = 0.49\ (\pm 0.21)\ \mathrm{k\Omega}$. This value is a factor of 9 smaller than the average nanowire resistance, although the surface of the growth substrate consists of oxidized InP, while in the nanowire case the STM tip touches an Au–In nanoparticle. Thus, the actual resistance of the tip–sample point contact in the nanowire case is expected to be significantly below 0.5 kΩ.

In a further reference measurement, we evaporated a ~10 nm Au film onto a highly doped InAs substrate and annealed it in UHV at 280 °C for 5 min, resulting in the formation of Au–In islands with a diameter of about 100 nm, which is comparable to the size of the metal nanoparticles on top of the nanowires. We imaged these Au–In islands by STM and then established point contacts between the STM tip and individual islands, thus simulating the situation of the nanowire point contact measurements, only excluding the resistance of the nanowires themselves. A very small average resistance of $R = 21.6\ (\pm 1.4)$ Ω was obtained, which can be regarded as the intrinsic resistance of our measurement setup, including all series resistances of the STM tip and sample connections, the sample back contact, and even the point contact between the STM probe tip and a metal particle. Thus, the kΩ-range resistance measured of individual nanowires can be attributed to the nanowire itself.

dx.doi.org/10.1021/nl402570u | Nano Lett. 2013, 13, 5182–5189

Complementary to the highly doped InP nanowires, another nanowire sample was investigated containing nonintentionally doped InAs nanowires with diameters of about 100 nm. Resistance measurements on 10 individual nanowires are shown in Figure 4b, all obtained from linear $I-V$ curves acquired with the STM probe tip in point contact. The average resistance of these nanowires is $R = 4.3\ (\pm 2.3) \times 10^5\ \Omega$, which is 100 times larger than for the highly doped InP nanowires. This complementary data set demonstrates the generality of our method to characterize nanowires of different materials and with orders of magnitude difference in resistivity.

It should be noted that both material systems studied here, InAs as well as highly doped InP, form Ohmic contacts with In–Au alloys, of which the metal particles on top of the nanowires consist. There are other nanowire systems like GaAs, which are known to form Schottky barriers toward their Au-based metal particles, even though those interfaces have shown much higher conductivity than comparable bulk Schottky barriers.[28,46] Contacting the metal particle of such nanowires by the STM tip can therefore not provide direct resistance measurements of the nanowire itself but instead investigate the $I-V$ properties of the highly interesting nanoscale interface. Indeed, with this method it has been possible to measure the Schottky barrier height between GaAs nanowires and their catalytic Au particles, as will be shown elsewhere.[47]

A unique advantage of the present method is the well-controlled formation of a point contact between the probe tip and the semiconductor nanowire with very low resistance (less than 22 Ω). Compared with other nanoprobe setups, the very clean environment of the STM operated at UHV conditions without any electron beams, together with STM probe tips being cleaned in vacuum and as-grown samples that are free of processing-induced contamination, is highly beneficial for the reproducible formation of Ohmic contacts to the nanowires.[36,48,49] The high resolution of the STM in imaging semiconductor nanostructures[50−52] ensures that the tip-nanowire point contact can be formed exactly at a specific position. Additionally, the in situ sputtered STM tips, as shown in Figure 2b, exhibit a much smaller radius of curvature than typical nanoprobes used elsewhere,[30,33] enabling very accurate imaging of objects with as high aspect ratios as upright-standing nanowires, as can be seen in Figure 1b. As a result, our STM-based method provides a significantly more precise positioning of the probe tip in respect to the center of the nanowire than what can be achieved in SEM. This is even more remarkable since our setup uses a single, standard STM, without the need for any complementary microscopy techniques, which would make the entire method more delicate, complicated, and expensive.

Finally, we will discuss our method in respect to conventional resistivity measurements on individual nanowires in the FET geometry using EBL-defined contacts. Although such measurements are well established, they rely on approximations made for interpretation of the results,[26,27] and they imply elaborate sample preparation and processing steps, which are not only time-consuming and expensive, but also expose the nanowires to aggressive environments like strong electron beams and chemical etching. Consequently, the reproducibility and quality of EBL-defined nanowire contacts is still a major challenge: When a set of individual nanowire devices is contacted, usually only a fraction of them shows reasonable device characteristics, often enough the formation of Ohmic contacts is not possible at all, as it was the case in our reference experiment, Figure 4c, while the majority of all our attempts to contact an individual nanowire with the STM tip from top resulted in reproducible $I-V$ curves with Ohmic contacts. Furthermore, studies with EBL-defined contacts often show a large spread of the resistance measured for individual nanowires,[22] often more than an order of magnitude larger than with our method. For certain types of more involved measurements and specific nanowires the $I-V$ results can be improved in accuracy[25,53] and have also been complemented by scanning gate microscopy data[54−56] or other scanning probe studies.[57,58] However, even with the best EBL-defined contacts the contact resistance still significantly influences the measured resistance of the entire device.[23,24] In contrast, the STM-based method can be applied to as-grown nanowires without any processing steps. Although STM in general is not a fast technique, the time needed for preparing and measuring nanowire samples until significant statistics on nanowire $I-V$ properties are obtained is comparable in both approaches.

In conclusion, we have successfully demonstrated how advanced device characterization is possible on general nanowire samples using nothing more than a standard STM. We image upright standing nanowires on-top, enabling us to very accurately position the STM tip as nanoprobe, and form a point contact with the nanowire. Ohmic contacts with an extremely low contact resistance of less than 22 Ω could reproducibly be established by this method for different nanowire material systems and doping levels, already indicating the versatility of this method. The very direct approach using as-grown nanowires without aggressive or elaborate sample processing allows the characterization also of very sensitive samples. On the other hand, it is possible to monitor the $I-V$ properties of individual nanowires during various stages of device processing in a realistic upright standing configuration. With the highly controllable conditions of a UHV-based STM chamber, the new method is also well suited to investigate how surface modifications like cleaning, oxidation, passivation, or more advanced surface chemistry will change the transport properties of individual nanowires. A first demonstration of comparing the $I-V$ properties of more complex upright-standing nanowires before and after chemical treatment is shown in Figure 1 of the Supporting Information. Furthermore, the comparatively simple and compact setup using a conventional STM without any further microscopy tools makes this method affordable, flexible, and even suitable for transport measurements at extreme conditions. Ultralow temperatures in the milliKelvin range, for example, are nowadays accessible by STM,[59] but not by SEM, TEM, or similar techniques. All these advantages make the new method presented here to a unique tool for nondestructively measuring resistivity and transport properties of a broad range of semiconductor nanowires and nanowire devices with high reproducibility, accuracy, and versatility.

■ ASSOCIATED CONTENT

Supporting Information

The $I-V$ spectra of upright-standing InP p-n-junction nanowires before and after surface cleaning by annealing under atomic hydrogen background. This material is available free of charge via the Internet at http://pubs.acs.org.

dx.doi.org/10.1021/nl402570u | Nano Lett. 2013, 13, 5182−5189

AUTHOR INFORMATION

Corresponding Author

*E-mail: Rainer.Timm@sljus.lu.se. Homepage: http://www.nano.lu.se/rainer.timm.

Present Addresses

[†]A.F. is also at MATERIALS - Institute for Surface Technologies and Photonics, Joanneum Research, Franz-Pichler-Str. 30, 8160 Weiz, Austria.

[‡]Institute for X-ray Physics, University of Göttingen, Friedrich-Hund-Platz 1, 37077 Göttingen, Germany.

Author Contributions

The manuscript was written through contributions of all authors. All authors have given approval to the final version of the manuscript.

Notes

The authors declare no competing financial interest.

ACKNOWLEDGMENTS

This work was performed within the Nanometer Structure Consortium at Lund University (nmC@LU), and was supported by the Swedish Research Council (VR), the Swedish Foundation for Strategic Research (SSF), the Swedish Energy Agency, the Crafoord Foundation, the Knut and Alice Wallenberg Foundation, and the European Research Council under the European Union's Seventh Framework Programme, Grant Agreement 259141. The authors want to thank Mubashar Irfan for supporting measurements and Dan Csontos for helpful discussion. One of the authors (R.T.) acknowledges support from the European Commission under the Marie Curie Intra-European Fellowship "NanowireDeviceSTM".

REFERENCES

(1) Lieber, C. M.; Wang, Z. L. Functional Nanowires. *MRS Bull.* **2007**, *32*, 99.

(2) Wallentin, J.; Anttu, N.; Asoli, D.; Huffman, M.; Åberg, I.; Magnusson, M. H.; Siefer, G.; Fuss-Kailuweit, P.; Dimroth, F.; Witzigmann, B.; Xu, H. Q.; Samuelson, L.; Deppert, K.; Borgström, M. T. InP Nanowire Array Solar Cells Achieving 13.8% Efficiency by Exceeding the Ray Optics Limit. *Science* **2013**, *339*, 1057.

(3) Nguyen, H. P. T.; Zhang, S.; Cui, K.; Han, X.; Fathololoumi, S.; Couillard, M.; Botton, G. A.; Mi, Z. p-Type Modulation Doped InGaN/GaN Dot-in-a-Wire White-Light-Emitting Diodes Monolithically Grown on Si(111). *Nano Lett.* **2011**, *11*, 1919.

(4) Gorji Ghalamestani, S.; Johansson, S.; Borg, B. M.; Lind, E.; Dick, K. A.; Wernersson, L.-E. Uniform and position-controlled InAs nanowires on 2″ Si substrates for transistor applications. *Nanotechnology* **2012**, *23*, 015302.

(5) Mourik, V.; Zuo, K.; Frolov, S. M.; Plissard, S. R.; Bakkers, E. P. A. M.; Kouwenhoven, L. P. Signatures of Majorana Fermions in Hybrid Superconductor-Semiconductor Nanowire Devices. *Science* **2012**, *336*, 1003.

(6) Deng, M. T.; Yu, C. L.; Huang, G. Y.; Larsson, M.; Caroff, P.; Xu, H. Q. Anomalous Zero-Bias Conductance Peak in a Nb-InSb Nanowire-Nb Hybrid Device. *Nano Lett.* **2012**, *12*, 6414.

(7) Bulgarini, G.; Reimer, M. E.; Hocevar, M.; Bakkers, E. P. A. M.; Kouwenhoven, L. P.; Zwiller, V. Avalanche amplification of a single exciton in a semiconductor nanowire. *Nat. Photonics* **2012**, *6*, 455.

(8) Ahtapodov, L.; Todorovic, J.; Olk, P.; Mjåland, T.; Slåttnes, P.; Dheeraj, D. L.; van Helvoort, A. T. J.; Fimland, B.-O.; Weman, H. A Story Told by a Single Nanowire: Optical Properties of Wurtzite GaAs. *Nano Lett.* **2012**, *12*, 6090.

(9) Björk, M. T.; Ohlsson, B. J.; Sass, T.; Persson, A. I.; Thelander, C.; Magnusson, M. H.; Deppert, K.; Wallenberg, L. R.; Samuelson, L. One-dimensional Steeplechase for Electrons Realized. *Nano Lett.* **2002**, *2*, 87.

(10) Wallentin, J.; Persson, J. M.; Wagner, J. B.; Samuelson, L.; Deppert, K.; Borgström, M. T. High-Performance Single Nanowire Tunnel Diodes. *Nano Lett.* **2010**, *10*, 974.

(11) Mårtensson, T.; Svensson, C. P. T.; Wacaser, B. A.; Larsson, M. W.; Seifert, W.; Deppert, K.; Gustafsson, A.; Wallenberg, L. R.; Samuelson, L. Epitaxial III-V Nanowires on Silicon. *Nano Lett.* **2004**, *4*, 1987.

(12) Samuelson, L. Self-forming nanoscale devices. *Mater. Today* **2003**, *6* (10), 22.

(13) Sköld, N.; Karlsson, L. S.; Larsson, M. W.; Pistol, M.-E.; Seifert, W.; Trägårdh, J.; Samuelson, L. Growth and Optical Properties of Strained GaAs–$Ga_xIn_{1-x}P$ Core-Shell Nanowires. *Nano Lett.* **2005**, *5*, 1943.

(14) Simpkins, B. S.; Pehrsson, P. E.; Laracuente, A. R. Electronic conduction in GaN nanowires. *Appl. Phys. Lett.* **2006**, *88*, 072111.

(15) Allen, J. E.; Perea, D. E.; Hemesath, E. R.; Lauhon, L. J. Nonuniform Nanowire Doping Profiles Revealed by Quantitative Scanning Photocurrent Microscopy. *Adv. Mater.* **2009**, *21*, 3067.

(16) Hjort, M.; Wallentin, J.; Timm, R.; Zakharov, A. A.; Andersen, J. N.; Samuelson, L.; Borgström, M. T.; Mikkelsen, A. Doping profile of InP nanowires directly imaged by photoemission electron microscopy. *Appl. Phys. Lett.* **2011**, *99*, 233113.

(17) Cai, W.; Che, Y.; Pelz, J. P.; Hemesath, E. R.; Lauhon, L. J. Direct Measurements of Lateral Variations of Schottky Barrier Height Across "End-On" Metal Contacts to Vertical Si Nanowires by Ballistic Electron Emission Microscopy. *Nano Lett.* **2012**, *12*, 694.

(18) Storm, K.; Halvardsson, F.; Heurlin, M.; Lindgren, D.; Gustafsson, A.; Wu, P. M.; Monemar, B.; Samuelson, L. Spatially resolved Hall effect measurement in a single semiconductor nanowire. *Nat. Nanotechnol.* **2012**, *7*, 718.

(19) Cui, Y.; Duan, X.; Hu, J.; Lieber, C. M. Doping and Electrical Transport in Silicon Nanowires. *J. Phys. Chem. B* **2000**, *104*, 5213.

(20) Scheffler, M.; Nadj-Perge, S.; Kouwenhoven, L. P.; Borgström, M. T.; Bakkers, E. P. A. M. Diameter-dependent conductance of InAs nanowires. *J. Appl. Phys.* **2009**, *106*, 124303.

(21) Léonard, F.; Talin, A. A. Electrical contacts to one- and two-dimensional nanomaterials. *Nat. Nanotechnol.* **2011**, *6*, 773.

(22) Suyatin, D. B.; Thelander, C.; Björk, M. T.; Maximov, I.; Samuelson, L. Sulfur passivation for ohmic contact formation to InAs nanowires. *Nanotechnology* **2007**, *18*, 105307.

(23) Zhang, Z.; Yao, K.; Liu, Y.; Jin, C.; Liang, X.; Chen, Q.; Peng, L.-M. Quantitative Analysis of Current-Voltage Characteristics of Semiconducting Nanowires: Decoupling of Contact Effects. *Adv. Funct. Mater.* **2007**, *17*, 2478.

(24) Hayden, O.; Björk, M. T.; Schmid, H.; Riel, H.; Drechsler, U.; Karg, S. F.; Lörtscher, E.; Riess, W. Fully Depleted Nanowire Field-Effect Transistor in Inversion Mode. *Small* **2007**, *3*, 230.

(25) Park, H.; Beresford, R.; Ha, R.; Choi, H.-J.; Shin, H.; Xu, J. Evaluation of metal-nanowire electrical contacts by measuring contact end resistance. *Nanotechnology* **2012**, *23*, 245201.

(26) Wunnicke, O. Gate capacitance of back-gated nanowire field-effect transistors. *Appl. Phys. Lett.* **2006**, *89*, 083102.

(27) Khanal, D. R.; Wu, J. Gate Coupling and Charge Distribution in Nanowire Field Effect Transistors. *Nano Lett.* **2007**, *7*, 2778.

(28) Léonard, F.; Talin, A. A.; Swartzentruber, B. S.; Picraux, S. T. Diameter-Dependent Electronic Transport Properties of Au-Catalyst/Ge-Nanowire Schottky Diodes. *Phys. Rev. Lett.* **2009**, *102*, 106805.

(29) Talin, A. A.; Léonard, F.; Swartzentruber, B. S.; Wang, X.; Hersee, S. D. Unusually Strong Space-Charge-Limited Current in Thin Wires. *Phys. Rev. Lett.* **2008**, *101*, 076802.

(30) Talin, A. A.; Léonard, F.; Katzenmeyer, A. M.; Swartzentruber, B. S.; Picraux, S. T.; Toimil-Molares, M. E.; Cederberg, J. G.; Wang, X.; Hersee, S. D.; Rishinaramangalum, A. Transport characterization in nanowires using an electrical nanoprobe. *Semicond. Sci. Technol.* **2010**, *25*, 024015.

(31) Katzenmeyer, A. M.; Léonard, F.; Talin, A. A.; Wong, P.-S.; Huffaker, D. L. Poole-Frenkel Effect and Phonon-Assisted Tunneling in GaAs Nanowires. *Nano Lett.* **2010**, *10*, 4935.

(32) Salehzadeh, O.; Chen, M. X.; Kavanagh, K. L.; Watkins, S. P. Rectifying characteristics of Te-doped GaAs nanowires. *Appl. Phys. Lett.* **2011**, *99*, 182102.
(33) Zhao, S.; Salehzadeh, O.; Alagha, S.; Kavanagh, K. L.; Watkins, S. P.; Mi, Z. Probing the electrical transport properties of intrinsic InN nanowires. *Appl. Phys. Lett.* **2013**, *102*, 073102.
(34) Hasegawa, Y.; Lyo, I.-W.; Avouris, P. Measurement of surface state conductance using STM point contacts. *Surf. Sci.* **1996**, *357*−*358*, 32.
(35) Hansen, K.; Nielsen, S. K.; Brandbyge, M.; Lægsgaard, E.; Stensgaard, I.; Besenbacher, F. Current-voltage curves of gold quantum point contacts revisited. *Appl. Phys. Lett.* **2000**, *77*, 708.
(36) Larsson, M. W.; Wallenberg, L. R.; Persson, A. I.; Samuelson, L. Probing of Individual Semiconductor Nanowhiskers by TEM-STM. *Microsc. Microanal.* **2004**, *10*, 41.
(37) Zhang, Z. Y.; Jin, C. H.; Liang, X. L.; Chen, Q.; Peng, L.-M. Current-voltage characteristics and parameter retrieval of semiconducting nanowires. *Appl. Phys. Lett.* **2006**, *88*, 073102.
(38) Zhao, J.; Sun, H.; Dai, S.; Wang, Y.; Zhu, J. Electrical Breakdown of Nanowires. *Nano Lett.* **2011**, *11*, 4647.
(39) Fian, A.; Lexholm, M.; Timm, R.; Mandl, B.; Håkanson, U.; Hessman, D.; Lundgren, E.; Samuelson, L.; Mikkelsen, A. New Flexible Toolbox for Nanomechanical Measurements with Extreme Precision and at Very High Frequencies. *Nano Lett.* **2010**, *10*, 3893.
(40) Wallentin, J.; Borgström, M. T. Doping of semiconductor nanowires. *J. Mater. Res.* **2011**, *26*, 2142.
(41) Wallentin, J.; Mergenthaler, K.; Ek, M.; Wallenberg, L. R.; Samuelson, L.; Deppert, K.; Pistol, M.-E.; Borgström, M. T. Probing the Wurtzite Conduction Band Structure Using State Filling in Highly Doped InP Nanowires. *Nano Lett.* **2011**, *11*, 2286.
(42) The linearity of the $I-V$ curve is determined by the residual of a linear least-squares fit over an voltage interval from −0.4 to +0.4 V.
(43) Dayeh, S. A.; Susac, D.; Kavanagh, K. L.; Yu, E. T.; Wang, D. Field Dependent Transport Properties in InAs Nanowire Field Effect Transistors. *Nano Lett.* **2008**, *8*, 3114.
(44) Hjort, M.; Wallentin, J.; Timm, R.; Zakharov, A. A.; Håkanson, U.; Andersen, J. N.; Lundgren, E.; Samuelson, L.; Borgström, M. T.; Mikkelsen, A. Surface Chemistry, Structure, and Electronic Properties from Microns to the Atomic Scale of Axially Doped Semiconductor Nanowires. *ACS Nano* **2012**, *6* (11), 9679.
(45) Hanrath, T.; Korgel, B. A. Chemical Surface Passivation of Ge Nanowires. *J. Am. Chem. Soc.* **2004**, *126*, 15466.
(46) Han, N.; Wang, F.; Yip, S.; Hou, J. J.; Xiu, F.; Shi, X.; Hui, A. T.; Hung, T.; Ho, J. C. GaAs nanowire Schottky barrier photovoltaics utilizing Au-Ga alloy catalytic tips. *Appl. Phys. Lett.* **2012**, *101*, 013105.
(47) Suyatin, D. B.; Jain, V.; Nebol'sin, V. A.; Trägårdh, J.; Messing, M. E.; Wagner, J. B.; Persson, O.; Timm, R.; Mikkelsen, A.; Maximov, I.; Samuelson, L.; Pettersson, H. Strong Schottky barrier reduction at Au-catalyst/GaAs-nanowire interfaces by electric dipole formation and Fermi level unpinning. Unpublished work, 2013.
(48) Beinik, I.; Kratzer, M.; Wachauer, A.; Wang, L.; Lechner, R. T.; Teichert, C.; Motz, C.; Anwand, W.; Brauer, G.; Chen, X. Y.; Hsu, X. Y.; Djurišić, A. B. Electrical properties of ZnO nanorods studied by conductive atomic force microscopy. *J. Appl. Phys.* **2011**, *110*, 052005.
(49) Bakkers, E. P. A. M.; van Dam, J. A.; de Franceschi, S.; Kouwenhoven, L. P.; Kaiser, M.; Verheijen, M.; Wondergem, H.; van der Sluis, P. Epitaxial growth of InP nanowires on germanium. *Nat. Mater.* **2004**, *3*, 769.
(50) Timm, R.; Eisele, H.; Lenz, A.; Ivanova, L.; Vossebürger, V.; Warming, T.; Bimberg, D.; Farrer, I.; Ritchie, D. A.; Dähne, M. Confined States of Individual Type-II GaSb/GaAs Quantum Rings Studied by Cross-Sectional Scanning Tunneling Spectroscopy. *Nano Lett.* **2010**, *10*, 3972.
(51) Kawasaki, J.; Timm, R.; Delaney, K. T.; Lundgren, E.; Mikkelsen, A.; Palmstrom, C. J. Local Density of States and Interface Effects in Semimetallic ErAs Nanoparticles Embedded in GaAs. *Phys. Rev. Lett.* **2011**, *107*, 036806.
(52) Hjort, M.; Lehmann, S.; Knutsson, J.; Timm, R.; Jacobsson, D.; Lundgren, E.; Dick, K. A.; Mikkelsen, A. Direct Imaging of Atomic Scale Structure and Electronic Properties of GaAs Wurtzite and Zinc Blende Nanowire Surfaces. *Nano Lett.* **2013**, *13* (9), 4492−4498.
(53) Borgström, M. T.; Norberg, E.; Wickert, P.; Nilsson, H. A.; Trägårdh, J.; Dick, K. A.; Statkute, G.; Ramvall, P.; Deppert, K.; Samuelson, L. Precursor evaluation for in situ InP nanowire doping. *Nanotechnology* **2008**, *19* (44), 445602.
(54) Gudiksen, M. S.; Lauhon, L. J.; Wang, J.; Smith, D. C.; Lieber, C. M. Growth of nanowire superlattice structures for nanoscale photonics and electronics. *Nature* **2002**, *415*, 617.
(55) Zhou, X.; Dayeh, S. A.; Wang, D.; Yu, E. T. Scanning gate microscopy of InAs nanowires. *Appl. Phys. Lett.* **2007**, *90*, 233118.
(56) Martin, D.; Heinzig, A.; Grube, M.; Geelhaar, L.; Mikolajick, T.; Riechert, H.; Weber, W. M. Direct Probing of Schottky Barriers in Si Nanowire Schottky Barrier Field Effect Transistors. *Phys. Rev. Lett.* **2011**, *107*, 216807.
(57) Koren, E.; Berkovitch, N.; Azriel, O.; Boag, A.; Rosenwaks, Y.; Hemesath, E. R.; Lauhon, L. J. Direct measurement of nanowire Schottky junction depletion region. *Appl. Phys. Lett.* **2011**, *99*, 223511.
(58) Menges, F.; Riel, H.; Stemmer, A.; Gotsmann, B. Quantitative Thermometry of Nanoscale Hot Spots. *Nano Lett.* **2012**, *12*, 596.
(59) Song, Y. J.; Otte, A. F.; Shvarts, V.; Zhao, Z.; Kuk, Y.; Blankenship, S. R.; Band, A.; Hess, F. M.; Stroscio, J. A. A 10 mK Scanning Probe Microscopy Facility. *Rev. Sci. Instrum.* **2010**, *81*, 121101.